GPAM mediated lysophosphatidic acid synthesis regulates mitochondrial dynamics in acute myeloid leukemia

入船, 秀俊

Received: 2 February 2023 | Revised: 13 April 2023 | Accepted: 19 April 2023

DOI: 10.1111/cas.15835

Cancer Science WILEY

ORIGINAL ARTICLE

GPAM mediated lysophosphatidic acid synthesis regulates mitochondrial dynamics in acute myeloid leukemia

Hidetoshi Irifune[1] | Yu Kochi[1] | Toshihiro Miyamoto[2] | Teppei Sakoda[1,3] | Koji Kato[1,3] | Yuya Kunisaki[1,3] | Koichi Akashi[1,3] | Yoshikane Kikushige[1,3]

[1]Department of Medicine and Biosystemic Sciences, Kyushu University Graduate School of Medicine, Fukuoka, Japan

[2]Department of Hematology, Faculty of Medicine, Institute of Medical Pharmaceutical and Health Sciences, Kanazawa University, Ishikawa, Japan

[3]Center for Cellular and Molecular Medicine, Kyushu University Hospital, Fukuoka, Japan

Correspondence
Koichi Akashi, Department of Medicine and Biosystemic Sciences, Kyushu University Graduate School of Medicine, 3-1-1 Maidashi, Higashi-ku, Fukuoka 812-8582, Japan.
Email: akashi.koichi.357@m.kyushu-u.ac.jp

Funding information
Ministry of Education, Culture, Sports, Science and Technology, Grant/Award Number: a Grant-in-Aid for Scientific Research (A) / 21407, a Grant-in-Aid for Scientific Research (B) / 21385 and a Grant-in-Aid for Scientific Research (B) / 22494

Abstract

Metabolic alterations, especially in the mitochondria, play important roles in several kinds of cancers, including acute myeloid leukemia (AML). However, AML-specific molecular mechanisms that regulate mitochondrial dynamics remain elusive. Through the metabolite screening comparing $CD34^+$ AML cells and healthy hematopoietic stem/progenitor cells, we identified enhanced lysophosphatidic acid (LPA) synthesis activity in AML. LPA is synthesized from glycerol-3-phosphate by glycerol-3-phosphate acyltransferases (GPATs), rate-limiting enzymes of the LPA synthesis pathway. Among the four isozymes of GPATs, glycerol-3-phosphate acyltransferases, mitochondrial (GPAM) was highly expressed in AML cells, and the inhibition of LPA synthesis by silencing GPAM or FSG67 (a GPAM-inhibitor) significantly impaired AML propagation through the induction of mitochondrial fission, resulting in the suppression of oxidative phosphorylation and the elevation of reactive oxygen species. Notably, inhibition of this metabolic synthesis pathway by FSG67 administration did not affect normal human hematopoiesis in vivo. Therefore, the GPAM-mediated LPA synthesis pathway from G3P represents a critical metabolic mechanism that specifically regulates mitochondrial dynamics in human AML, and GPAM is a promising potential therapeutic target.

KEYWORDS
acute myeloid leukemia, GPAM, lysophosphatidic acid, mitochondrial dynamics, oxidative phosphorylation

Abbreviations: AML, acute myeloid leukemia; BM, bone marrow; CB, umbilical cord blood; CE-TOFMS, capillary electrophoresis-connected electrospray ionization time-of-flight mass spectroscopy; DMSO, dimethyl sulfoxide; DRP1, dynamin-related protein 1; FACS, fluorescence-activated cell sorting; FAO, fatty acid oxidation; FCCP, carbonyl cyanide 4-trifluoromethoxy-phenylhydrazone; G3P, glycerol-3-phosphate; GPAM, glycerol-3-phosphate acyltransferase mitochondrial; GPAT, glycerol-3-phosphate acyltransferase; HSPC, hematopoietic stem/progenitor cells; LDs, lipid droplets; LPA, lysophosphatidic acid; MMP, mitochondrial membrane potential; mtDNA, mitochondrial DNA; NAC, N-acetylcysteine; NSG, NOD. Cg-Prkdc^{scid} Il2rg^{tm1Wjl}/SzJ; OCR, oxygen consumption rate; OXPHOS, oxidative phosphorylation; PI, propidium iodide; ROS, reactive oxygen species; RT-qPCR, real-time quantitative polymerase chain reaction; Scr, scrambled shRNA control; shRNA, short hairpin RNA; TEM, transmission electron microscopy; TMRE, tetramethylrhodamine ethyl ester; β2-M, beta-2-microglobulin.

1 | INTRODUCTION

Acute myeloid leukemia is a genetically heterogeneous aggressive hematological malignancy characterized by clonal expansion of abnormal immature myeloid cells. Despite recent advances in therapeutic approaches, AML is associated with a poor prognosis owing to the high incidence of relapse and severe treatment-related toxicity.[1–3] Therefore, the development of novel, effective, and safe therapeutic strategies is highly required.

Cancer cells mainly rely on anaerobic glycolysis for energy generation, a phenomenon known as the Warburg effect.[4] However, several kinds of cancer, including AML, strongly depend on OXPHOS rather than anaerobic glycolysis for their survival.[5–9] Mitochondrial function, reliance on OXPHOS, and regulation of ROS considerably differ between AML and normal hematopoietic cells, providing a rationale for therapeutic applications targeting mitochondrial metabolism in AML.[10–13] Consistently, the combination therapy of venetoclax, a BCL-2 inhibitor with hypomethylating agent azacitidine targeting OXPHOS, improved the overall survival of patients with AML who were ineligible for standard induction therapy.[14,15] Furthermore, novel therapeutic models targeting mitochondrial metabolism in AML by inhibiting the mitochondrial complex, protein translocation, proteases, and pyrimidine biosynthesis have been reported.[6,10–12,16] Thus, targeting mitochondrial metabolism represents a novel and targeted therapeutic approach in AML.

Mitochondrial dynamics and lipid metabolism coordinately play pivotal roles in the maintenance of cancer-specific mitochondrial function.[10,17,18] Mitochondria are highly dynamic organelles that divide and fuse continuously to respond to metabolic demands and oxidative stress. Imbalances between mitochondrial fission and fusion contribute to the dysregulation of apoptosis, cell proliferation, and ROS production. Mitochondrial dynamics imbalances are related to the initiation, progression, and chemoresistance of several malignant tumors, including AML.[8,17–21] Furthermore, alterations in lipid metabolism activities are also observed in cancer and have attracted attention as a target for cancer-specific metabolism.[22,23] In AML, lipid metabolic reprogramming contributes to disease progression and confers resistance to chemotherapies, including venetoclax.[21,24–28] Thus, mitochondrial dynamics and lipid metabolic pathways are involved in the pathogenesis of AML by modifying mitochondrial functions. However, the molecules that specifically govern mitochondrial dynamics and lipid metabolism in AML have not been well elucidated.

This study aimed to identify AML-specific molecules involved in the regulation of mitochondrial function. Primary $CD34^+$ AML cells strongly activated the LPA synthesis pathway. GPAM (also known as GPAT1), a rate-limiting enzyme of the LPA synthesis pathway, was specifically expressed in primary $CD34^+$ AML cells but not in normal $CD34^+$ HSPCs. Inhibition of GPAM-mediated LPA biosynthesis strongly inhibited the propagation and self-renewal potentials of human AML cells by suppressing mitochondrial membrane dynamics and OXPHOS activity without affecting normal hematopoiesis. Collectively, these results suggest that LPA synthesis from G3P by key enzyme GPAM, plays a critical role in maintaining mitochondrial function and represents a promising therapeutic target for AML.

2 | MATERIALS AND METHODS

2.1 | Cell lines and primary cell culture

Details of the experiments are described in Appendix S1.

2.2 | Metabolite analysis

$CD34^+$ cells were isolated from the CB or BM using the Indirect CD34 MicroBead Kit (Miltenyi Biotec) according to the manufacturer's instructions. Metabolite extraction was performed according to the manual of Human Metabolome Technologies. Metabolites were analyzed using CE-TOFMS systems (C-Scope, Human Metabolome Technologies). More details about the experiments are described in our previous study.[29]

2.3 | FACS analysis

Details of the experiments are described in Appendix S1.

2.4 | Knockdown of GPAM using shRNA

For GPAM knockdown, lentivirus vectors containing shRNA targeting human GPAM and scrambled control sequences were purchased from VectorBuilder Inc. (VB180824-1060qzm, VB180824-1062qxz, VB180824-1063qtf, and VB151023-10034).

HEK293T cells were transfected with PAX2 (Addgene), VSV-G (Addgene), and lentiviral vectors using polyethyleneimine (Polysciences). Lentiviral supernatants were harvested at 48 and 72 h post transfection and concentrated by ultracentrifugation at 570,000 *g* for 2 h at 4°C. Leukemic cell lines were plated in 12-well plates (1.0×10^5 cells/well) with a medium supplemented with 8 mg/mL polybrene (Sigma-Aldrich) and spin infected at 300 *g* for 2 h at 37°C. Cells were treated after 24 h with puromycin to select transduced cells.

2.5 | Protein lysate preparation and Western blotting

Details of the experiments are described in Appendix S1.

2.6 | mRNA and mtDNA quantification by qPCR

Details of the experiments are described in Appendix S1.

2.7 | Mitochondrial mass, MMP, cellular ROS, and LDs staining

Details of the experiments are described in Appendix S1.

2.8 | Transmission electron microscopy

Non-viable cells were removed using a dead cell removal kit (Miltenyi Biotec) before fixation. THP-1 and $CD34^+$ cells from AML patients were fixed in 2.5% glutaraldehyde and 0.1 M sucrose. Cells were post-fixed in 1% osmic acid, dehydrated with a graded ethanol series, and embedded in Epon812. Ultrathin 80 nm sections were cut by Leica EM UC7, stained with 2% uranyl acetate and Sato's Pb, and then examined with a Tecnai F20. Quantification of the mitochondrial length (major axis) and the area was performed using ImageJ software version 1.52q (NIH). A random selection of mitochondria derived from leukemic cells ($n = 15$ cells/group) was analyzed for each experiment.

2.9 | XFp seahorse analyzer

Details of the experiments are described in Appendix S1.

2.10 | Xenotransplantation

Details of the experiments are described in Appendix S1.

2.11 | Statistical analysis

All statistical analyses were performed using JMP software. Statistical significance was set at $p < 0.05$. Differences between the two groups were assessed using the Wilcoxon rank-sum test or unpaired Student's *t*-test. The Kaplan–Meier plot was used for the xenotransplantation, and the difference in overall survival was determined using the log-rank test. The level of significance is indicated as follows: $^*p < 0.05$; $^{**}p < 0.01$; $^{***}p < 0.001$; n.s. $p > 0.05$.

3 | RESULTS

3.1 | Human AML cells activate the LPA synthesis pathway from G3P by GPAM

To identify the metabolic pathways on which AML cells specifically depend, we comprehensively analyzed 116 intracellular metabolites of $CD34^+$ AML cells or $CD34^+$ HSPCs from healthy donors using a mass spectrometer. We identified several differentially expressed metabolites between AML cells and healthy HSPCs (details are reported in our previous study[29]). Among these, G3P was significantly decreased in $CD34^+$ AML cells compared with healthy $CD34^+$ HSPCs (Figure 1A, $p < 0.05$). G3P is an intermediate metabolite of glycolysis and a substrate of triacylglycerol and phospholipids (Figure S1A). The rate-limiting step of the glycerophospholipid biosynthesis pathway is the production of LPA from G3P, which is mediated by GPATs.[30,31] We first evaluated the mRNA expression levels of different GPAT isozymes between $CD3^+$ T cells and $CD34^+$ AML blasts in the BM of 13 patients with AML (Table S1) using RT-qPCR. Among the four GPAT isozymes, only GPAM was highly expressed in the $CD34^+$ AML blasts (Figure 1B). Intracellular flow cytometry analysis revealed highly expressed GPAM in primary $CD34^+$ AML blasts (Figure 1C), whereas healthy $CD34^+$ HSPCs (Figure 1D) and mature $CD3^+$ T cells purified from identical patients with AML (Figure S1B) exhibited considerably lower GPAM expression levels. These results suggest that primary human AML cells actively consume G3P and activate LPA synthesis by increased expression of GPAM.

3.2 | Inhibition of LPA synthesis via GPAM knockdown attenuates AML propagation in vitro and in vivo

To determine whether GPAM is involved in the pathogenesis of AML, we knocked down GPAM in AML cell lines, including THP-1, MOLM-13, Kasumi-1, and OCI-AML3. AML cell lines were transduced with shRNAs targeting GPAM or scrambled control sequences. Suppression of GPAM was confirmed by Western blotting (Figure 2A and Figure S2A) and RT-qPCR (Figure S2B). GPAM knockdown significantly suppressed the proliferation of all the cell lines examined (Figure 2B). To assess the role of GPAM in vivo, THP-1 cells with GPAM knockdown or scrambled sequences were transplanted into sublethally irradiated NSG mice (Figure S2C). GPAM knockdown strongly inhibited the reconstitution potential of THP-1 cells in mouse BM 28 days after xenotransplantation (Figure 2C). Consequently, GPAM knockdown significantly prolonged the survival of the recipient mice (Figure 2D). Collectively, these data demonstrate that GPAM is required for AML propagation, both in vitro and in vivo.

3.3 | GPAM plays a pivotal role in the regulation of mitochondrial membrane dynamics, OXPHOS, and redox homeostasis in human AML cells

GPAM regulates mitochondrial metabolism by promoting mitochondrial fusion and OXPHOS.[32,33] We, therefore, tested whether GPAM knockdown affects the mitochondrial function of THP-1 cells by evaluating mitochondrial mass and MMP. GPAM knockdown significantly reduced the mitochondrial mass and MMP, as evaluated by Mito-Tracker (Figure 3A,B) and TMRE staining (Figure S3A), respectively. We also quantified mtDNA, a proxy for mitochondrial mass,[34,35] and confirmed that mtDNA content (the

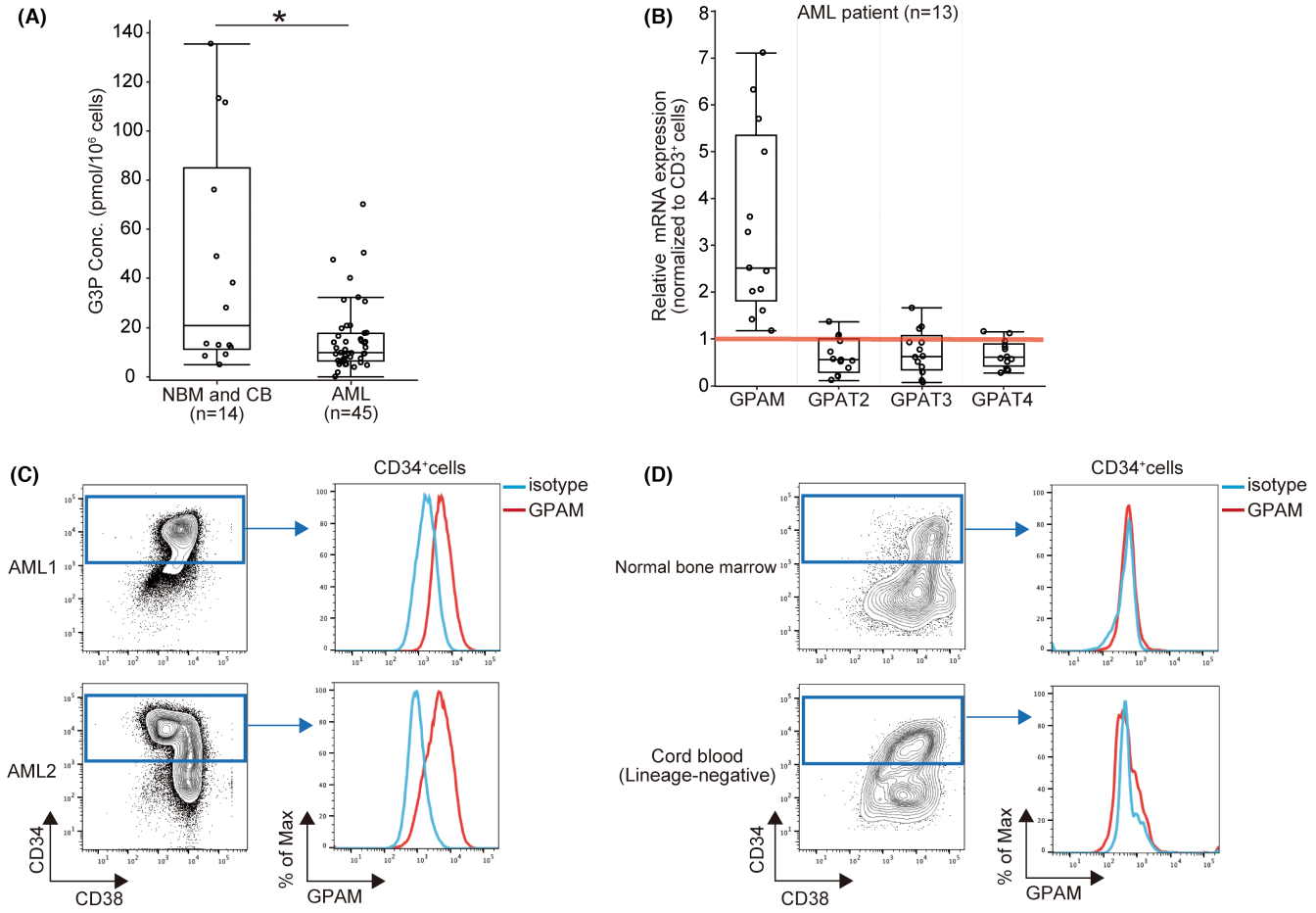

FIGURE 1 (A) Capillary electrophoresis-connected electrospray ionization time-of-flight mass spectroscopy (CE-TOFMS) analyses showing G3P levels in healthy CD34$^+$ hematopoietic stem/progenitor cells (HSPCs) ($n=14$) and CD34$^+$ acute myeloid leukemia (AML) cells ($n=45$). p-values were calculated using Wilcoxon rank-sum test. * $p<0.05$. (B) RT-qPCR of mRNA expression levels of GPAT isozymes in CD34$^+$ cells of the bone marrow (BM) of patients with AML ($n=13$). β2-M was used as an internal control. The mRNA expression levels of GPATs were normalized to those of CD3$^+$ cells in each patient sample. (C, D) Representative FACS plots of intracellular GPAM expression levels in CD34$^+$ AML cells (C) and healthy CD34$^+$ HSPCs (BM of healthy donors and umbilical cord blood [CB]; [D]).

ratio of mtDNA to nuclear DNA) was reduced by GPAM knockdown (Figure S3B). TEM revealed that GPAM knockdown significantly reduced the size of the mitochondria (Figure 3C,D and Figure S3C), suggesting that GPAM promotes mitochondrial fusion in human AML cells. We next sought to test whether GPAM knockdown suppressed cellular growth of AML via inducing mitochondrial fission. Since DRP1 is essential for mitochondrial fission,[36] we treated THP-1 cells with Mdivi-1 (a DRP1 inhibitor). Mdivi-1 partially rescued the growth suppression and mitochondrial division of THP-1 cells by GPAM knockdown (Figure 3E,F). Furthermore, it has been shown that mitochondrial fusion increases the efficiency of ATP production, whereas mitochondrial fission promotes ROS production.[37] We next evaluated OXPHOS activity and ROS levels. GPAM knockdown significantly suppressed mitochondrial ATP production (Figure 3G and Figure S3D-F) and increased cellular ROS levels (Figure 3H,I) in THP-1 cells. Overall, these results suggest that GPAM plays a pivotal role in the regulation of mitochondrial membrane dynamics, OXPHOS, and redox homeostasis in human AML cells.

3.4 | FSG67 exerts antileukemic effects by inducing mitochondrial fission

FSG67, a mitochondrial GPAT inhibitor, was originally developed as a drug to treat obesity and diabetes.[38-40] FSG67 was designed to mimic the phosphate of G3P and saturated long-chain of palmitoyl-CoA. This compound reduces the production of LPA, a precursor of triacylglycerol and phospholipids, by inhibiting the acylation of G3P with long-chain acyl-CoA.

We first evaluated the antileukemic effects of FSG67 in vitro. FSG67 induced apoptosis and growth inhibition of THP-1 and MOLM-13 cells (Figure S4A,B) in a dose-dependent manner. Then, we compared the viability of normal hematopoietic cells (healthy CD34$^+$ HSPCs and CD3$^+$ T cells) and primary CD34$^+$ AML cells after 48 h of FSG67 treatment. FSG67 induced apoptosis of primary AML cells with little effect on healthy HSPCs and T cells in vitro (Figure 4A). Importantly, after 4 h of FSG67 treatment, viable THP-1 cells exhibited reduced mitochondrial mass (Figure S4C,D), MMP (Figure S4E), and mtDNA content (Figure S4F), resulting in suppression of OCR

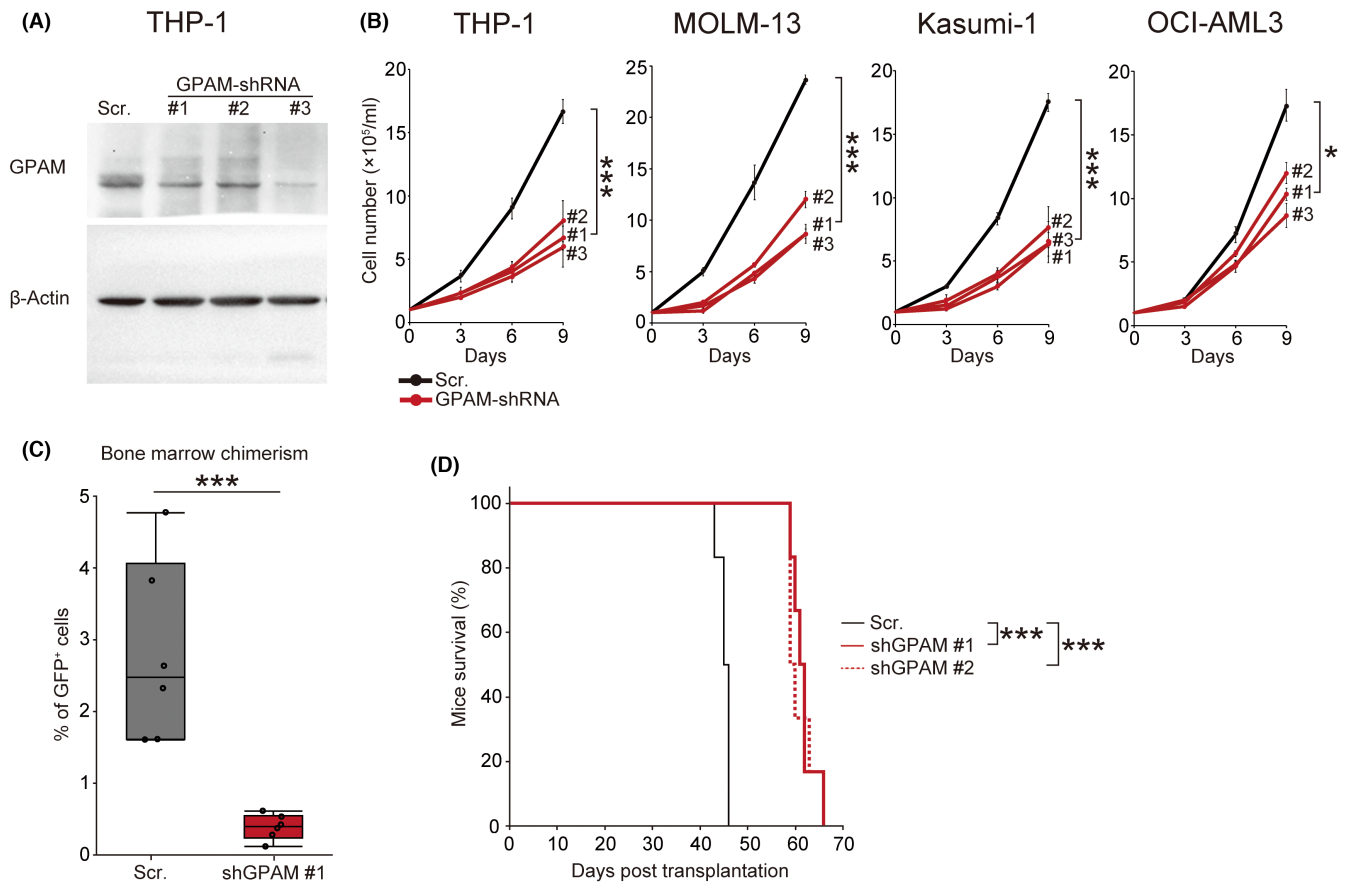

FIGURE 2 (A) Representative Western blot images showing the knockdown efficiency of shRNA targeting GPAM in THP-1 cells. β-actin was used as a loading control. (B) Cell growth curves of acute myeloid leukemia (AML) cell lines transfected with shRNA targeting GPAM or scrambled control. Data are represented as mean ± SD. (C) Frequency of green fluorescent protein positive (GFP^+) cells in the bone marrow (BM) of NSG mice 28 days after xenotransplantation of THP-1 cells. (D) The Kaplan–Meier survival curves of NSG mice after xenotransplantation of THP-1 cells. *p*-values were calculated using Student's *t*-test (B), Wilcoxon rank-sum test (C), or log-rank Mantel-Cox test (D). $^*p < 0.05$, $^{***}p < 0.001$.

(Figure S4G), similar to those in the GPAM knockdown experiments. Analysis of the mitochondrial ultrastructure by TEM demonstrated that the mitochondria in primary $CD34^+$ AML cells treated with FSG67 became more fragmented and lost a clear cristae structure compared with those in the control (Figure 4B,C), suggesting that FSG67 induced mitochondrial fission in primary AML cells. Consistent with mitochondrial fission, we observed a reduction in mitochondrial mass (Figure 4D,E), MMP (Figure S4H), and OXPHOS activity (Figure 4F,G) in primary $CD34^+$ AML cells treated with FSG67. In addition, the antileukemic effect and mitochondrial division induced by FSG67 was rescued with DRP1 inhibition (Figure 4H and Figure S4I).

Furthermore, FSG67 inhibited the accumulation of LDs in THP-1 and primary $CD34^+$ AML cells (Figure 4I,J and Figure S4J), as evaluated by BODIPY staining. LD-derived fatty acids fuel mitochondrial ATP production, and AML cells actively utilize FAO to meet metabolic demands.[24-26,41] Mito Fuel Flex Test, which determines the rate of oxidation of each fuel, including glucose, glutamine, and fatty acids, demonstrated that THP-1 cells treated with FSG67 completely failed to utilize fatty acids for mitochondrial energy production. In contrast, glutamine dependency was slightly increased in the presence of FSG67, presumably reflecting the compensatory energy production from glutamine (Figure 4K). Moreover, as with GPAM knockdown, FSG67 treatment led to increased ROS levels, and the ROS scavenger NAC almost completely inhibited ROS production in THP-1 and primary AML cells (Figure 4L and Figure S4K-M). Collectively, these results suggest that FSG67 induces mitochondrial fission, leading to impaired OXPHOS activity and increased ROS production in AML cells.

3.5 | Lysophosphatidic acid synthesis by GPAM is required for the maintenance of mitochondrial function of AML cells

GPAM synthesizes LPA from G3P and acyl-CoA; therefore, we investigated whether the antileukemic effect of GPAM inhibition results from the suppression of LPA synthesis in AML cells. LPA is an amphipathic phospholipid present both intra- and extracellularly.[42] Exogenous LPA supplementation to culture media alleviated the growth inhibition induced by FSG67 (Figure 5A) and GPAM knockdown (Figure S5A) in THP-1 cells. Exogenous LPA also prevented the induction of apoptosis by FSG67 in THP-1 cells and improved the cell viability of primary AML cells treated with FSG67 (Figure 5B).

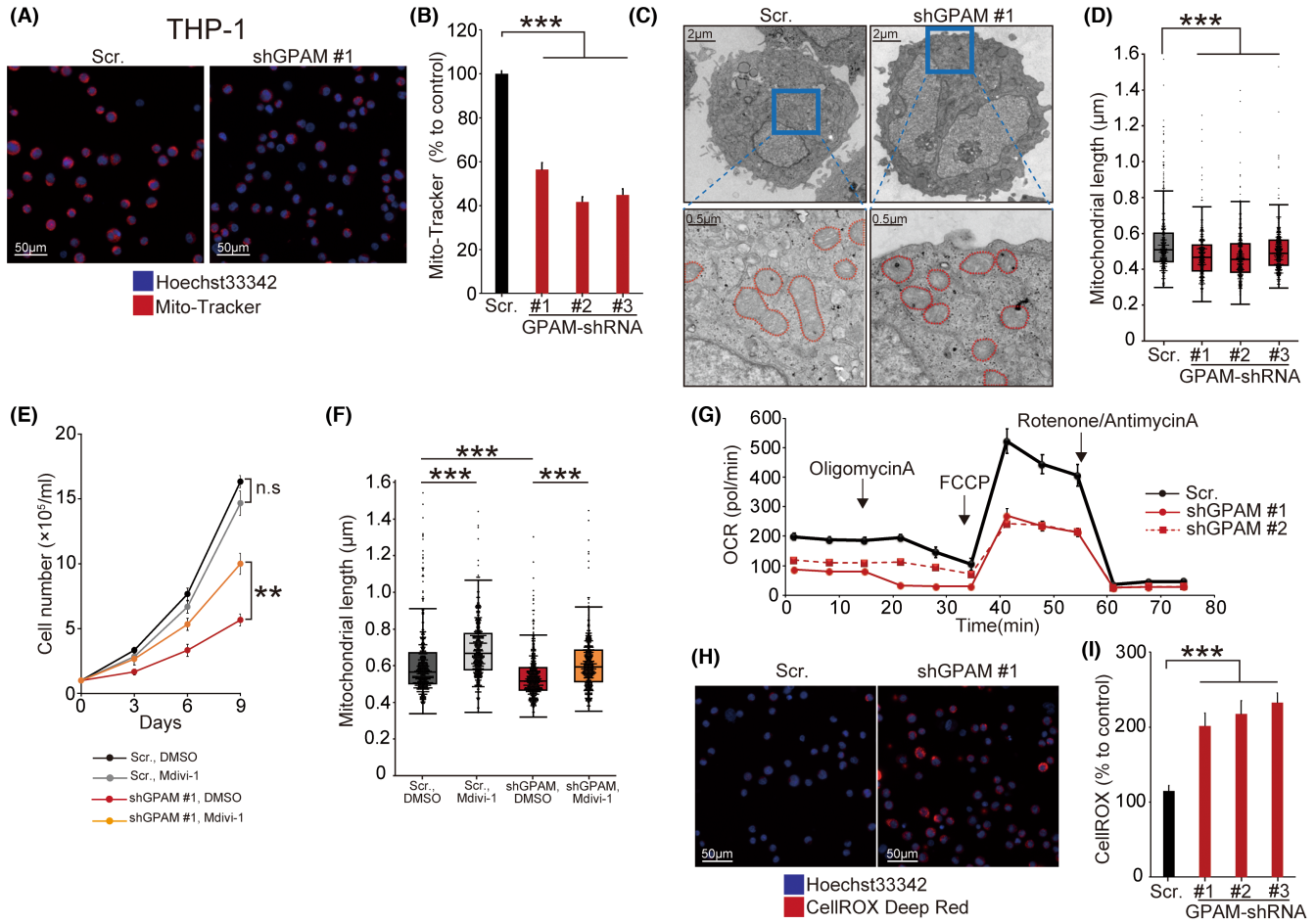

FIGURE 3 (A) Representative fluorescent images showing the mitochondria in THP-1 cells transfected with shRNA targeting GPAM or scrambled control taken by Cellomics ArrayScan VTI HCS Reader. Nuclei were stained with Hoechst 33342 (blue), and mitochondria were stained with Mito-Tracker Deep Red (red). (B) Quantification of Mito-Tracker images by Cellomics ArrayScan VTI HCS Reader. The mean fluorescence intensity values were normalized to those of the untreated control. (C) Representative transmission electron microscopy (TEM) images showing the mitochondria in THP-1 cells transfected with shRNA targeting GPAM or control. Red dotted lines outline the individual mitochondria. (D) TEM analysis of the lengths of 300–450 mitochondria derived from a random selection of THP-1 cells transfected with shRNA targeting GPAM or control. (E) Cellular growth of THP-1 cells transfected with shRNA targeting GPAM or control in the presence or absence of Mdivi-1. (F) TEM analysis of the lengths of 300–450 mitochondria derived from a random selection of THP-1 cells transfected with shRNA targeting GPAM or control treated with DMSO or Mdivi-1 for 4 h. (G) Seahorse extracellular flux analysis of basal and stressed oxygen consumption rates (OCRs) in THP-1 cells transfected with shRNA targeting GPAM or control. (H) Representative fluorescent images showing the reactive oxygen species (ROS) in THP-1 cells transfected with shRNA targeting GPAM or control taken by Cellomics ArrayScan VTI HCS Reader. Nuclei were stained with Hoechst 33342 (blue), and ROS were stained with CellROX Deep Red (red). (I) Quantification of CellROX Deep Red by Cellomics ArrayScan VTI HCS Reader. Data are represented as mean ± SD. *p*-values were calculated using an unpaired Student's *t*-test (B, E, I) or Wilcoxon rank-sum test (D, F). $^{*}p<0.05$; $^{**}p<0.01$; $^{***}p<0.001$.

Furthermore, LPA supplementation rescued the suppression of mitochondrial mass (Figure 5C-E), MMP (Figure S5B), mtDNA copy numbers (Figure S5C), and OCR (Figure 5F) induced by FSG67 in THP-1 and primary AML cells.

3.6 | GPAM inhibition by FSG67 represents an effective treatment strategy for AML in vivo

We evaluated the effects of FSG67 on AML in vivo. THP-1 cells were injected into sublethally irradiated NSG mice. Five days after injection, the mice transplanted with THP-1 cells were treated with DMSO or FSG67 (10 mg/kg or 20 mg/kg) once daily for 2 weeks. Mice treated with FSG67 displayed a reduced leukemic burden in the BM 28 days after xenotransplantation (Figure 6A) and a significantly prolonged overall survival (Figure 6B) compared with control mice.

We also evaluated the efficacy of FSG67 treatment in primary AML cells and normal hematopoiesis in vivo. Primary $CD34^{+}$ cells from three patients with AML and $CD34^{+}$ CB cells were injected into sublethally irradiated NSG mice. After confirmation of engraftment, recipient mice were treated with DMSO or FSG67 (20 mg/kg) once daily for 2 weeks (Figure S6A). Compared with the control, treatment with FSG67 reduced the leukemic burden in the BM (Figure 6C) and peripheral blood (Figure S6B) of mice 10 to

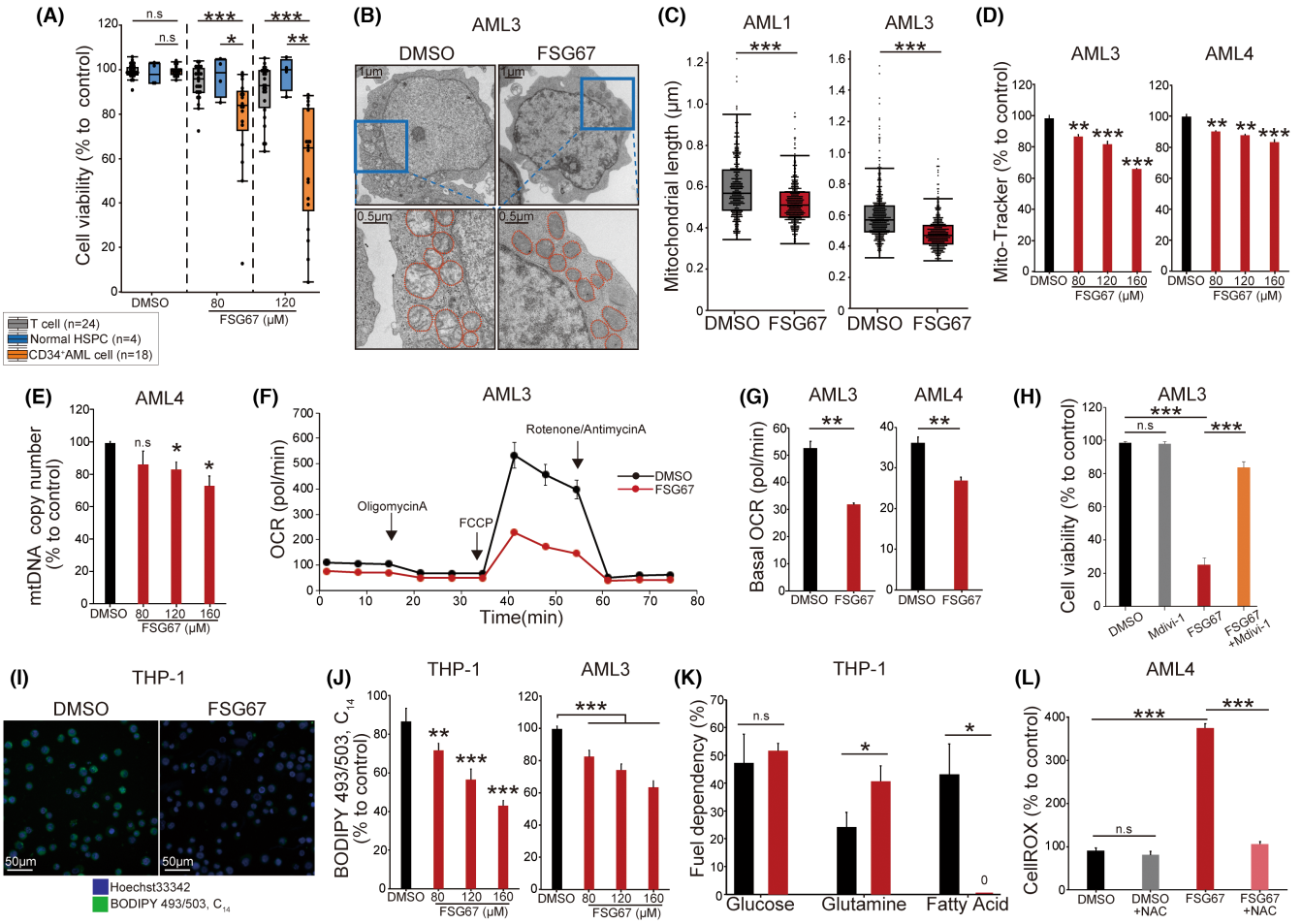

FIGURE 4 (A) Annexin V- and PI-based FACS analyses of the cell viabilities of $CD3^+$ cells ($n=24$), $CD34^+$ cells of umbilical cord blood (CB) ($n=4$) and $CD34^+$ acute myeloid leukemia (AML) cells ($n=18$) after 48 h of DMSO or FSG67 treatments. Each point represents the cell viability of the individual sample. (B) Representative transmission electron microscopy (TEM) images showing the mitochondria in $CD34^+$ AML cells treated with DMSO or FSG67 for 4 h. (C) TEM analysis of the lengths of 300–450 mitochondria derived from a random selection of primary $CD34^+$ AML cells treated with DMSO or FSG67 for 4 h. (D) FACS analysis of Mito-Tracker images in primary $CD34^+$ AML cells treated with DMSO or FSG67 for 4 h. (E) mtDNA copy numbers after 4 h of DMSO or FSG67 treatment were assessed by the measurement of the mitochondrial ND1 gene. Quantification of ND1 expression levels relative to the human globulin gene was assessed by qPCR. (F,G) Seahorse extracellular flux analysis of basal and stressed oxygen consumption rates (OCRs) in primary $CD34^+$ AML cells treated with DMSO or FSG67 for 4 h. (H) Annexin V- and PI-based FACS analyses of the viabilities of primary $CD34^+$ AML cells treated with DMSO or FSG67 in the presence or absence of Mdivi-1 for 48 h. (I) Representative fluorescence images showing the lipid droplets (LDs) in THP-1 cells treated with DMSO or FSG67 for 30 min. Nuclei were stained with Hoechst 33342 (blue), and LDs were stained with BODIPY 493/503. (J) Quantification of BODIPY 493/503 in THP-1 and primary $CD34^+$ AML cells treated with DMSO or FSG67 for 30 min. (K) Seahorse extracellular flux analysis of mitochondrial fuel dependencies of THP-1 cells treated with DMSO or FSG67 for 4 h. Fuel dependencies were measured by the addition of a first inhibitor (UK5099, BPTES, or etomoxir) and later a mixture of the other two inhibitors in each experiment. (L) Quantification of the CellROX Deep Red of primary $CD34^+$ AML cells treated with DMSO or FSG67 in the presence or absence of NAC for 4 h was analyzed by FACS. Data are represented as mean ± SD. *p*-values were calculated using Wilcoxon rank-sum test (A and C) or an unpaired Student's *t*-test (D, E, G, H, and J–L). $^*p<0.05$; $^{**}p<0.01$; $^{***}p<0.001$; n.s, $p>0.05$.

20 weeks after xenotransplantation. Furthermore, identical numbers of human $CD45^+$ cells from first recipient mice were harvested and serially transplanted into secondary recipient mice. Notably, the residual AML cells from FSG67-treated mice exhibited greatly reduced reconstitution potential in the BM (Figure 6D) and spleen (Figure S6C,D) of secondary recipients, suggesting that the self-renewing leukemic-repopulating cells were selectively eradicated by FSG67 treatment in vivo.

In contrast to AML cells, FSG67 treatment had no effect on reconstitution of hematopoietic cells in mice reconstituted with healthy $CD34^+$ HSPCs, and we observed comparable proportions of human $CD45^+$ cells in the BM (Figure 6E) and peripheral blood (Figure S6E) between the DMSO- and FSG67-treated groups. Moreover, FSG67 did not alter the frequency of human $CD34^+$ HSPCs (Figure 6F) or lineage-committed mature blood cells (Figure 6G). Collectively, our results demonstrate that GPAM inhibition by FSG67 represents an

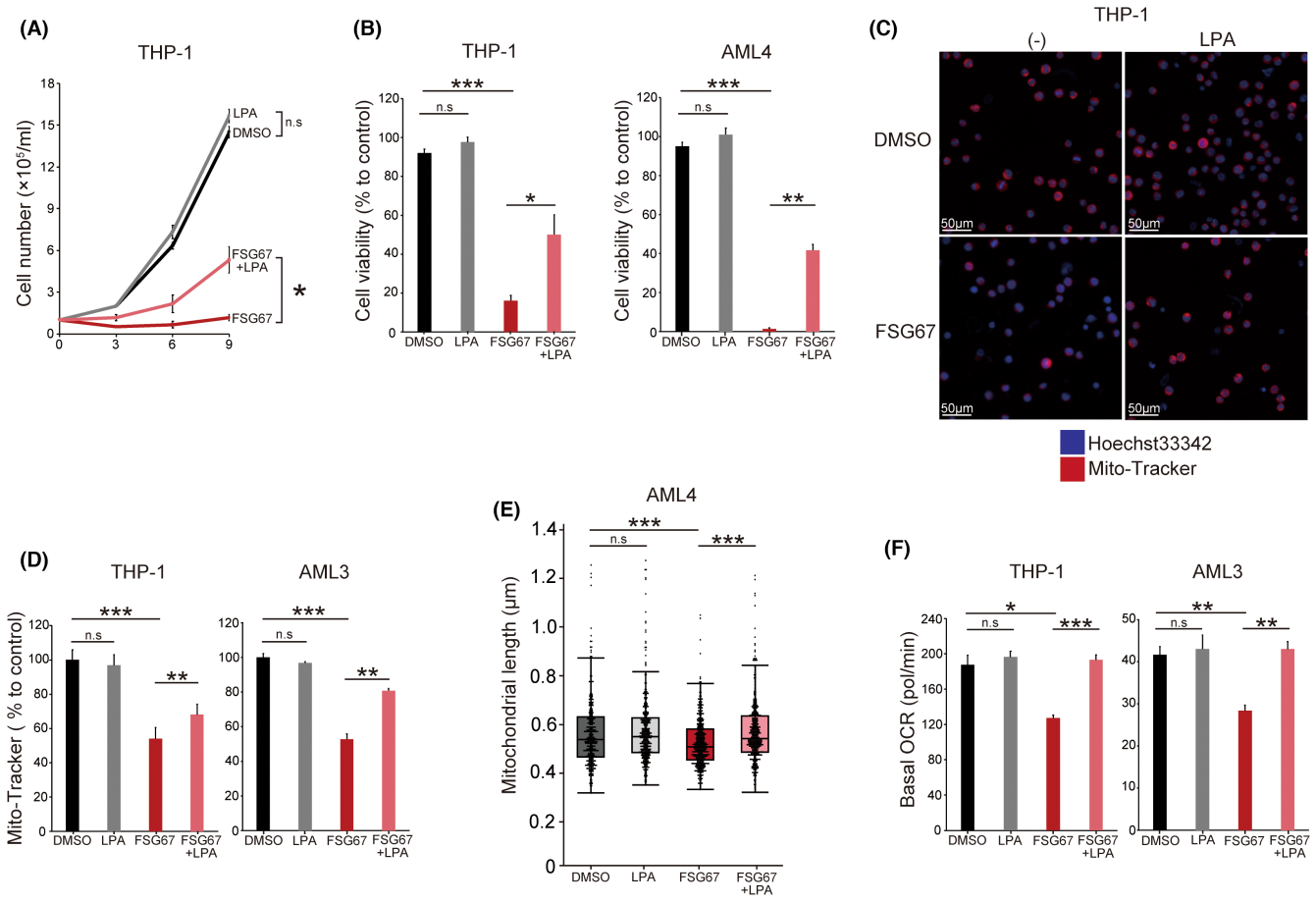

FIGURE 5 (A) Cell growth curves of THP-1 cells treated with DMSO or FSG67 in the presence or absence of lysophosphatidic acid (LPA). (B) Annexin V- and PI-based FACS analyses of the cell viabilities of THP-1 and primary CD34$^+$ acute myeloid leukemia (AML) cells treated with DMSO or FSG67 in the presence or absence of LPA for 48 h. (C) Representative fluorescent images showing the mitochondria in THP-1 cells treated with DMSO or FSG67 in the absence or presence of LPA for 4 h. Nuclei were stained with Hoechst 33342 (blue), and mitochondria were stained with Mito-Tracker Deep Red (red). (D) Quantification of the Mito-Tracker in THP-1 and primary CD34$^+$ AML cells treated with DMSO or FSG67 in the presence or absence of LPA for 4 h. (E) Transmission electron microscopy (TEM) analysis of the lengths of 300–450 mitochondria derived from a random selection of CD34$^+$ AML cells treated with DMSO or FSG67 in the presence or absence of LPA for 4 h. (F) Seahorse extracellular flux analysis of basal oxygen consumption rate (OCR) of THP-1 and primary CD34$^+$ AML cells treated with DMSO or FSG67 in the presence or absence of LPA for 4 h. Data are represented as mean ± SD. *p*-values were calculated using an unpaired Student's *t*-test (A, B, D, and F) or Wilcoxon rank-sum test (E). $^*p<0.05$; $^{**}p<0.01$; $^{***}p<0.001$; n.s, $p>0.05$.

effective treatment strategy for AML without affecting normal hematopoiesis in vivo.

4 | DISCUSSION

We identified GPAM as a novel therapeutic target and critical regulator of mitochondrial metabolism in human AML. Primary AML cells express high GPAM, whereas healthy HSPCs do not. GPAM knockdown resulted in suppressed leukemic growth, mitochondrial fusion, and OXPHOS activity, and increased ROS production in AML cells. FSG67, a GPAM inhibitor, impaired the proliferation and mitochondrial function of AML without affecting normal hematopoiesis. Exogenous LPA supplementation attenuated the antileukemic effect, suggesting that the GPAM-mediated LPA biosynthesis plays a critical role in maintaining mitochondrial dynamics and OXPHOS activity in human AML. (Figure 7).

Abnormalities in mitochondrial dynamics play pivotal roles in the initiation and progression of cancers, including AML.[43,44] The mitochondrial mass of AML cells tends to be larger than that of healthy HSPCs.[10,12] Furthermore, the mitochondrial fusion of AML cells increases OPXHOS and induces chemoresistance to cytarabine.[21] However, a therapeutic strategy targeting mitochondrial dynamics in AML has not yet been discovered, because no AML-specific molecules that regulate the mitochondria dynamics have been identified yet. Our study identified GPAM as an important regulator of mitochondrial fusion in AML cells. GPAM is a rate-limiting enzyme in the lipid biosynthesis pathway that synthesizes LPA on the mitochondrial outer membrane. Phospholipids constitute structural components of cellular membranes, and triacylglycerols are stored in LDs

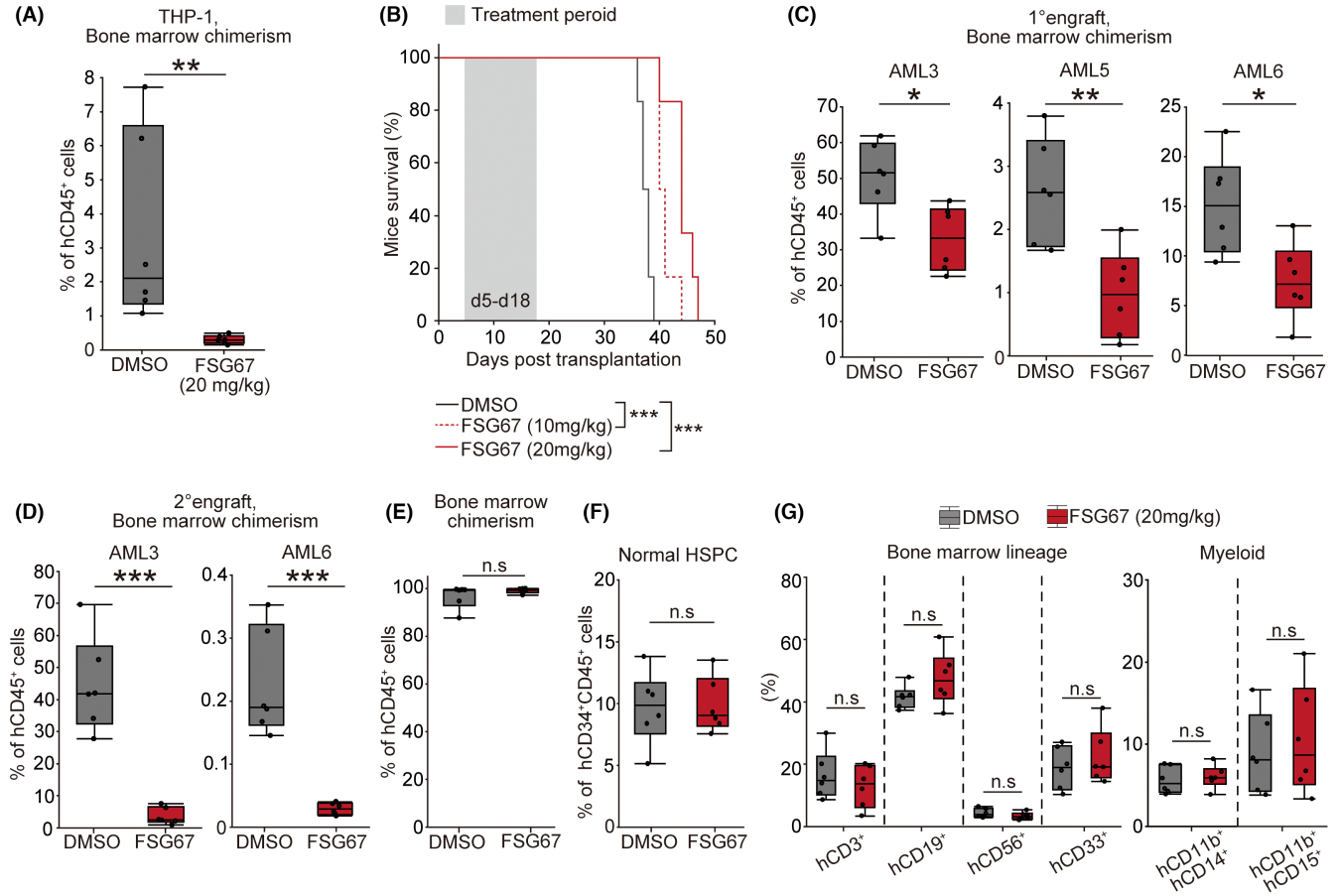

FIGURE 6 (A) Frequencies of human CD45$^+$ cells in the bone marrow (BM) of NSG mice ($n=6$ mice per group) 28 days after xenotransplantation of THP-1 cells (1.0×10^6 cells per mouse). Xenografted mice were treated with DMSO or FSG67 (20 mg/kg, i.p.) once daily for 2 weeks. (B) Kaplan–Meier survival curves of NSG mice ($n=6$ mice per group) after xenotransplantation of THP-1 cells. (C) Frequencies of human CD45$^+$ acute myeloid leukemia (AML) cells in the BM of NSG mice ($n=6$ mice per group) treated with DMSO or FSG67 (20 mg/kg, i.p., once daily for 2 weeks after engraftment) 10–20 weeks after xenotransplantation of human CD34$^+$ cells of AML patients. (D) Frequencies of human CD45$^+$ AML cells in the BM of secondary recipient NSG mice injected with human CD45$^+$ cells from first recipients (5.0×10^5 cells per mouse) after second transplantation. (E, F) Frequencies of human CD45$^+$ hematopoietic cells (E) and human CD34$^+$CD45$^+$ hematopoietic stem/progenitor cells (HSPCs) (F) in the BM of NSG mice (n = 6 mice per group) treated with DMSO or FSG67 (20 mg/kg, i.p., once daily for 2 weeks) 10 weeks after umbilical cord blood (CB) transplantation. (G) Proportions of B cells, T cells, NK cells, and myeloid cells in the BM of NSG mice ($n=6$ mice per group) treated with DMSO or FSG67 after CB transplantation. Myeloid cells were further classified by human CD11b, human CD14, and human CD15. p-values were calculated using the Wilcoxon rank-sum test (A and C–G) or log-rank Mantel–Cox test (B). *$p<0.05$; **$p<0.01$; ***$p<0.001$; n.s, $p>0.05$.

and utilized as energy resources during starvation. We demonstrated that GPAM inhibition suppresses LD accumulation, resulting in impaired FAO in AML cells. Moreover, consistent with recent studies showing that chemotherapy-resistant AML cells upregulate FAO to maintain high OXPHOS activity,[21,27,28] in the present study, FSG67 treatment exhibited potent antileukemic effects in patient-derived xenograft models transplanted with relapsed AML cells after allogeneic transplantation and AML cells with adverse genetic abnormalities. Thus, GPAM inhibition could be effective in patients with AML with poor prognosis by simultaneously suppressing both mitochondrial dynamics and lipid metabolism.

The current study indicates that GPAM regulates mitochondrial fusion by producing LPA. However, the downstream molecular mechanisms underlying GPAM-mediated mitochondrial fusion in AML remain unclear. DRP1 is an essential regulator of mitochondrial fission, which is activated on the mitochondrial outer membrane after oligomerization.[36,43] Intriguingly, phosphatidic acid, which can be synthesized from LPA, inhibits DRP1-mediated mitochondrial division.[45] On the other hand, DRP1 knockdown inhibited mitochondrial fragmentation induced by GPAM knockdown in HeLa cells.[32] These observations imply that modulators of mitochondrial dynamics, such as DRP1, could be involved in GPAM-mediated regulation of mitochondrial dynamics in human AML. Indeed, we believe that this is consistent with the fact that the antileukemic effect of GPAM inhibition was attenuated by Mdivi-1, a DRP1 inhibitor, in our study. Further studies are necessary to clarify the AML-specific molecular mechanisms.

Furthermore, regarding oxidative stress induced by FSG67, NAC almost completely suppressed the FSG67-induced ROS production, while the antileukemic effect of FSG67 was only partially rescued. These results suggested that the antileukemic effect of FSG67

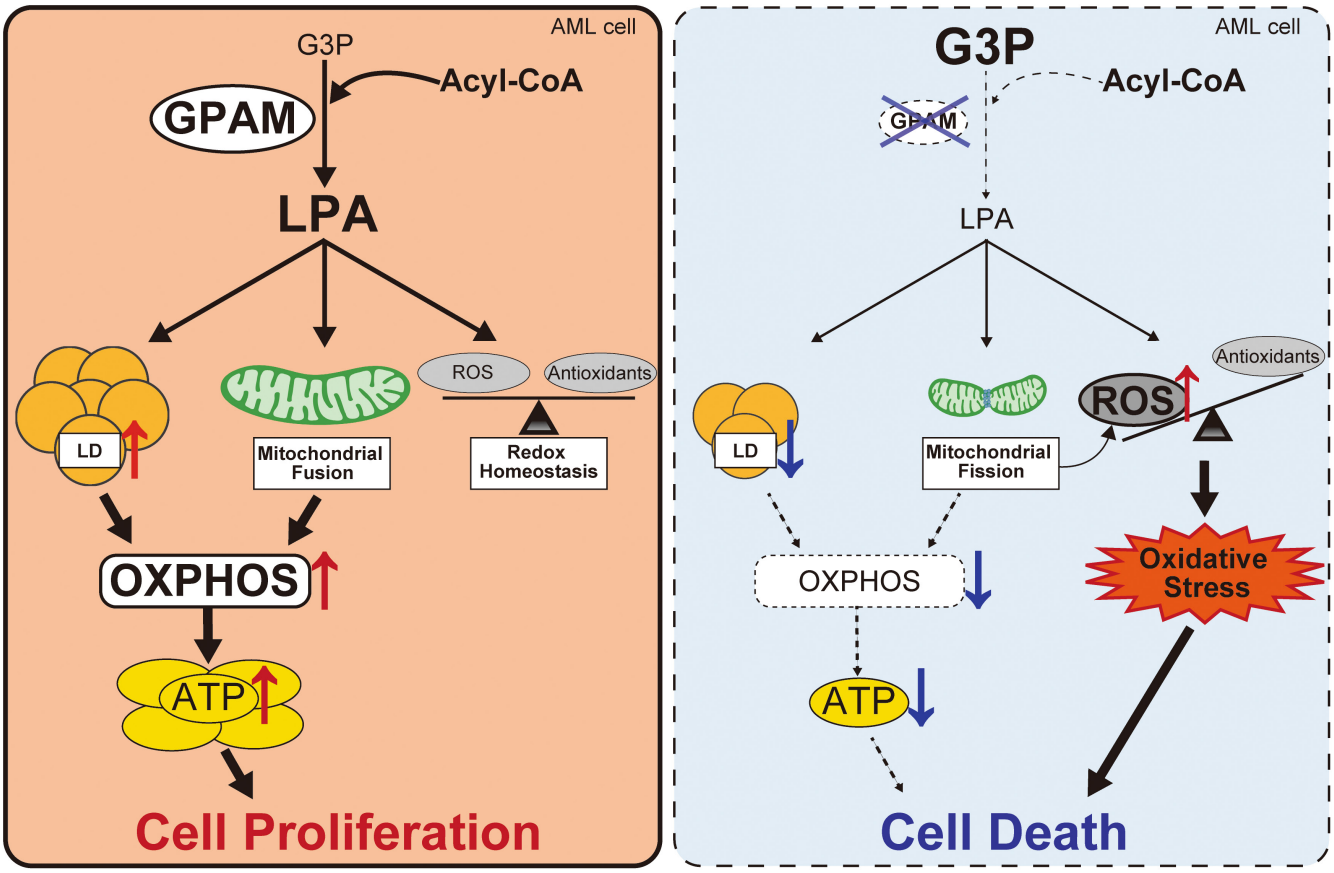

FIGURE 7 A schematic diagram of this study. AML, acute myeloid leukemia; LD, lipid droplets; LPA, lysophosphatidic acid; OXPHOS, oxidative phosphorylation; ROS, reactive oxygen species.

largely depended upon the reduction of OXPHOS and might be less affected by ROS. On the other hand, NAC is a precursor of glutathione, and glutathione requires glutamate, which is synthesized from glutamine, cysteine, and glycine. We found that AML cells after FSG67 treatment depended upon glutamine-derived OXPHOS. We, therefore, considered that NAC did not completely rescue cellular survival of AML in vitro, because NAC presumably promoted glutathione synthesis and consumed glutamine, resulting in the suppressed glutamine-derived OXPHOS activity after FSG67 treatment.

In summary, we identified GPAM as a novel regulator of mitochondrial metabolism in AML. This study suggests targeting GPAM as a promising therapeutic strategy against AML by suppressing the leukemia-specific mitochondrial function.

AUTHOR CONTRIBUTIONS

Contribution: H.I., Y.Ki., and Y.Ko. designed and performed all experiments, analyzed the data, performed the statistical analysis, and wrote the manuscript. T.M., T.S., K.K., and Y.Ku. analyzed the data. K.A. supervised the overall project and wrote the manuscript.

ACKNOWLEDGMENTS

We thank Yasuyuki Ohkawa of the Laboratory for Technical Support, Medical Institute of Bioregulation, Kyushu University for valuable help in performing the electron microscopic analysis.

FUNDING INFORMATION

This study was supported in part by a Grant-in-Aid for Scientific Research (A) to K.A. (No. 21407314) and a Grant-in-Aid for Scientific Research (B) to T.M. (No. 21385681) and to Y.Kikushige. (No. 22494899), from the Ministry of Education, Culture, Sports, Science and Technology of Japan.

CONFLICT OF INTEREST STATEMENT

Koichi Akashi is an Editorial Board Member of *Cancer Science* and received scholarship endowment from Otsuka Pharmaceutical Co. Ltd., Nippon Shinyaku Co. Ltd., TAIHO Phamaceutical Co. Ltd., Asahi Kasei Pharma Corporation, Kyowa Kirin Co. Ltd., CHUGAI PHARMACEUTICAL CO. LTD., Sumitomo Dainippon Pharma Co. Ltd., AbbVie Inc., Eisai Co. Ltd., and Takeda Pharmaceutical Co. Ltd. The other authors have no conflict of interest.

ETHICS STATEMENT

Approval of the research protocol by an Institutional Reviewer Board: The research was approved by the Institutional Reviewer Board of Kyushu University (Approval No. 2020–569).

Informed Consent: All informed consent was obtained according to the Kyushu Clinical sample Network (KCNET) (Approval No. 22102–00).

Registry and the Registration No. of the study/trial: N/A.

Animal Studies: The animal study was approved by the Ethics Committee of Kyushu University (Approval No. A-21-224-0).

ORCID

Hidetoshi Irifune https://orcid.org/0000-0001-9354-4661

REFERENCES

1. Papaemmanuil E, Gerstung M, Bullinger L, et al. Genomic classification and prognosis in acute myeloid leukemia. *N Engl J Med*. 2016;374(23):2209-2221.
2. Freeman SD, Hills RK, Virgo P, et al. Measurable residual disease at induction redefines partial response in acute myeloid leukemia and stratifies outcomes in patients at standard risk without NPM1 mutations. *J Clin Oncol*. 2018;36(15):1486-1497.
3. Perl AE, Martinelli G, Cortes JE, et al. Gilteritinib or chemotherapy for relapsed or refractory *FLT3*-mutated AML. *N Engl J Med*. 2019;381(18):1728-1740.
4. Warburg O. On the origin of cancer cells. *Science*. 1956;123(3191):309-314.
5. Baccelli I, Gareau Y, Lehnertz B, et al. Mubritinib targets the electron transport chain complex I and reveals the landscape of OXPHOS dependency in acute myeloid leukemia. *Cancer Cell*. 2019;36(1):84-99.
6. Molina JR, Sun Y, Protopopova M, et al. An inhibitor of oxidative phosphorylation exploits cancer vulnerability. *Nat Med*. 2018;24(7):1036-1046.
7. Roesch A, Vultur A, Bogeski I, et al. Overcoming intrinsic multidrug resistance in melanoma by blocking the mitochondrial respiratory chain of slow-cycling JARID1B(high) cells. *Cancer Cell*. 2013;23(6):811-825.
8. Bonnay F, Veloso A, Steinmann V, et al. Oxidative metabolism drives immortalization of neural stem cells during tumorigenesis. *Cell*. 2020;182(6):1490-1507.
9. Sancho P, Burgos-Ramos E, Tavera A, et al. MYC/PGC-1α balance determines the metabolic phenotype and plasticity of pancreatic cancer stem cells. *Cell Metab*. 2015;22(4):590-605.
10. Skrtić M, Sriskanthadevan S, Jhas B, et al. Inhibition of mitochondrial translation as a therapeutic strategy for human acute myeloid leukemia. *Cancer Cell*. 2011;20(5):674-688.
11. Cole A, Wang Z, Coyaud E, et al. Inhibition of the mitochondrial protease ClpP as a therapeutic strategy for human acute myeloid leukemia. *Cancer Cell*. 2015;27(6):864-876.
12. Sriskanthadevan S, Jeyaraju DV, Chung TE, et al. AML cells have low spare reserve capacity in their respiratory chain that renders them susceptible to oxidative metabolic stress. *Blood*. 2015;125(13):2120-2130.
13. Kuntz EM, Baquero P, Michie AM, et al. Targeting mitochondrial oxidative phosphorylation eradicates therapy-resistant chronic myeloid leukemia stem cells. *Nat Med*. 2017;23(10):1234-1240.
14. Pollyea DA, Stevens BM, Jones CL, et al. Venetoclax with azacitidine disrupts energy metabolism and targets leukemia stem cells in patients with acute myeloid leukemia. *Nat Med*. 2018;24(12):1859-1866.
15. DiNardo CD, Jonas BA, Pullarkat V, et al. Azacitidine and Venetoclax in previously untreated acute myeloid leukemia. *N Engl J Med*. 2020;383(7):617-629.
16. Sykes DB, Kfoury YS, Mercier FE, et al. Inhibition of dihydroorotate dehydrogenase overcomes differentiation blockade in acute myeloid leukemia. *Cell*. 2016;167(1):171-186.
17. Pei S, Minhajuddin M, Adane B, et al. AMPK/FIS1-mediated mitophagy is required for self-renewal of human AML stem cells. *Cell Stem Cell*. 2018;23(1):86-100.
18. Panina SB, Baran N, Brasil da Costa FH, Konopleva M, Kirienko NV. A mechanism for increased sensitivity of acute myeloid leukemia to mitotoxic drugs. *Cell Death Dis*. 2019;10(8):617.
19. Vyas S, Zaganjor E, Haigis MC. Mitochondria and cancer. *Cell*. 2016;166(3):555-566.
20. Schrepfer E, Scorrano L. Mitofusins, from mitochondria to metabolism. *Mol Cell*. 2016;61(5):683-694.
21. Farge T, Saland E, de Toni F, et al. Chemotherapy-resistant human acute myeloid leukemia cells are not enriched for leukemic stem cells but require oxidative metabolism. *Cancer Discov*. 2017;7(7):716-735.
22. Vriens K, Christen S, Parik S, et al. Evidence for an alternative fatty acid desaturation pathway increasing cancer plasticity. *Nature*. 2019;566(7744):403-406.
23. Cheng X, Geng F, Pan M, et al. Targeting DGAT1 ameliorates glioblastoma by increasing fat catabolism and oxidative stress. *Cell Metab*. 2020;32(2):229-242.
24. Ricciardi MR, Mirabilii S, Allegretti M, et al. Targeting the leukemia cell metabolism by the CPT1a inhibition: functional preclinical effects in leukemias. *Blood*. 2015;126(16):1925-1929.
25. Ye H, Adane B, Khan N, et al. Leukemic stem cells evade chemotherapy by metabolic adaptation to an adipose tissue niche. *Cell Stem Cell*. 2016;19(1):23-37.
26. Tabe Y, Yamamoto S, Saitoh K, et al. Bone marrow adipocytes facilitate fatty acid oxidation activating AMPK and a transcriptional network supporting survival of acute monocytic leukemia cells. *Cancer Res*. 2017;77(6):1453-1464.
27. Jones CL, Stevens BM, D'Alessandro A, et al. Inhibition of amino acid metabolism selectively targets human leukemia stem cells. *Cancer Cell*. 2018;34(5):724-740.
28. Stevens BM, Jones CL, Pollyea DA, et al. Fatty acid metabolism underlies venetoclax resistance in acute myeloid leukemia stem cells. *Nat Cancer*. 2020;1(12):1176-1187.
29. Kikushige Y, Miyamoto T, Kochi Y, et al. Human acute leukemia utilizes branched-chain amino acid catabolism to maintain stemness through regulating PRC2 function. *Blood Adv*. 2022. Online ahead of print.
30. Yu J, Loh K, Song ZY, Yang HQ, Zhang Y, Lin S. Update on glycerol-3-phosphate acyltransferases: the roles in the development of insulin resistance. *Nutr Diabetes*. 2018;8(1):34.
31. Karasawa K, Tanigawa K, Harada A, Yamashita A. Transcriptional regulation of acyl-CoA: glycerol-*sn*-3-phosphate acyltransferases. *Int J Mol Sci*. 2019;20(4):964.
32. Ohba Y, Sakuragi T, Kage-Nakadai E, et al. Mitochondria-type GPAT is required for mitochondrial fusion. *EMBO J*. 2013;32(9):1265-1279.
33. Faris R, Fan YY, De Angulo A, et al. Mitochondrial glycerol-3-phosphate acyltransferase-1 is essential for murine CD4(+) T cell metabolic activation. *Biochim Biophys Acta*. 2014;1842(10):1475-1482.
34. de Almeida MJ, Luchsinger LL, Corrigan DJ, Williams LJ, Snoeck HW. Dye-independent methods reveal elevated mitochondrial mass in hematopoietic stem cells. *Cell Stem Cell*. 2017;21(6):725-729.
35. Filippi MD, Ghaffari S. Mitochondria in the maintenance of hematopoietic stem cells: new perspectives and opportunities. *Blood*. 2019;133(18):1943-1952.
36. Fonseca TB, Sánchez-Guerrero Á, Milosevic I, Raimundo N. Mitochondrial fission requires DRP1 but not dynamins. *Nature*. 2019;570(7761):E34-E42.
37. Giacomello M, Pyakurel A, Glytsou C, Scorrano L. The cell biology of mitochondrial membrane dynamics. *Nat Rev Mol Cell Biol*. 2020;21(4):204-224.
38. Wydysh EA, Medghalchi SM, Vadlamudi A, Townsend CA. Design and synthesis of small molecule glycerol 3-phosphate acyltransferase inhibitors. *J Med Chem*. 2009;52(10):3317-3327.
39. Kuhajda FP, Aja S, Tu Y, et al. Pharmacological glycerol-3-phosphate acyltransferase inhibition decreases food intake and adiposity and increases insulin sensitivity in diet-induced obesity. *Am J Physiol Regul Integr Comp Physiol*. 2011;301(1):R116-R130.

40. McFadden JW, Aja S, Li Q, et al. Increasing fatty acid oxidation remodels the hypothalamic neurometabolome to mitigate stress and inflammation. *PLoS One*. 2014;9(12):e115642.
41. Bosc C, Broin N, Fanjul M, et al. Autophagy regulates fatty acid availability for oxidative phosphorylation through mitochondria-endoplasmic reticulum contact sites. *Nat Commun*. 2020;11(1):4056.
42. Meleh M, Pozlep B, Mlakar A, et al. Determination of serum lysophosphatidic acid as a potential biomarker for ovarian cancer. *J Chromatogr B Analyt Technol Biomed Life Sci*. 2007;858(1–2):287-291.
43. Archer SL. Mitochondrial dynamics — mitochondrial fission and fusion in human diseases. *N Engl J Med*. 2013;369(23):2236-2251.
44. Ma Y, Wang L, Jia R. The role of mitochondrial dynamics in human cancers. *Am J Cancer Res*. 2020;10(5):1278-1293.
45. Adachi Y, Itoh K, Yamada T, et al. Coincident phosphatidic acid interaction restrains Drp1 in mitochondrial division. *Mol Cell*. 2016;63(6):1034-1043.

SUPPORTING INFORMATION

Additional supporting information can be found online in the Supporting Information section at the end of this article.

How to cite this article: Irifune H, Kochi Y, Miyamoto T, et al. GPAM mediated lysophosphatidic acid synthesis regulates mitochondrial dynamics in acute myeloid leukemia. *Cancer Sci*. 2023;00:1-12. doi:10.1111/cas.15835